Acta Crystallographica Section B
Structural Science
ISSN 0108-7681

Crystal structures of the trifluoromethyl sulfonates $M(SO_3CF_3)_2$ (M = Mg, Ca, Ba, Zn, Cu) from synchrotron X-ray powder diffraction data

Robert Dinnebier, Natalia Sofina, Lars Hildebrandt and Martin Jansen*

Max-Planck-Institut für Festkörperforschung, Heisenbergstrasse 1, D-70569 Stuttgart, Germany

Correspondence e-mail: m.jansen@fkf.mpg.de

Received 24 November 2005
Accepted 14 March 2006

The crystal structures of divalent metal salts of trifluoromethyl sulfonic acid ('trifluoromethyl sulfonates') $M(SO_3CF_3)_2$ (M = Mg, Ca, Ba, Zn, Cu) were determined from high-resolution X-ray powder diffraction data. Magnesium, calcium and zinc trifluoromethyl sulfonate crystallize in the rhombohedral space group $R\bar{3}$. Barium trifluoromethyl sulfonate crystallizes in the monoclinic space group $I2/a(C2/c)$ and copper trifluoromethyl sulfonate crystallizes in the triclinic group $P\bar{1}$. Within the crystal structures the trifluoromethyl sulfonate anions are arranged in double layers with the apolar CF_3 groups pointing towards each other. The cations are located next to the SO_3 groups. The symmetry relations between the different crystal structures have been analysed.

1. Introduction

Owing to its amphiphilic character the trifluoromethyl sulfonate anion continues to attract much attention in various fields of basic research as well as in manifold technical applications. In chemical syntheses, $(SO_3CF_3)^-$ is utilized as a 'mild' leaving group (Umenoto *et al.*, 1990), while mixtures of its metal salts and free acids are effective catalysts for *e.g.* electrophilic aromatic substitutions (Mouhtady *et al.*, 2003) or cationic polymerizations (Sage *et al.*, 2004). The highest activity is presently displayed in the context of high-energy batteries, particularly lithium-ion batteries, where alkali, zinc or magnesium trifluoromethyl sulfonates are contained in some of the complex (gel) polymer electrolytes (McLin & Angell, 1992; Munshi *et al.*, 1989; Greenbaum, 1987; Semkow & Sammels, 1987; Forsyth *et al.*, 1997; Zheng *et al.*, 1998; Rhodes *et al.*, 1999, 2002; Ikeda, Mori, Furuhashi & Masuda, 1999; Ikeda, Mori, Furuhashi, Masuda & Yamamoto, 1999; Kumar & Munichandraiah, 2000*a*,*b*; Mitra *et al.*, 2001; Kumar & Sampath, 2003). Our interest in trifluoromethyl sulfonates originates from the various degrees of rotational freedom available to the anion in the solid state. This special feature makes this class of ionic solids an ideal system for studying the interplay of the paddle wheel (Kvist & Bengtzelius, 1973; Lundén, 1994) and volume effect (Secco, 1992, 1993), both of which enhance the translational cation mobility in rotator phases (Jansen, 1991).

In spite of the general importance of trifluoromethyl sulfonates, the crystal chemistry of the alkali metal trifluoromethyl sulfonates has been revealed only recently. Owing to the various structural phase transitions, no untwinned single crystals were available except for sodium (Sofina *et al.*, 2003) and potassium trifluoromethyl sulfonate (Korus & Jansen, 2001), and the crystal structures had to be solved using powder diffraction data (Tremayne *et al.*, 1992; Dinnebier *et al.*, 2004; Hildebrandt *et al.*, 2005). In addition to these structural

Table 1
Crystallographic data for magnesium, calcium, barium, zinc and copper trifluoromethyl sulfonate.

Formula	$Mg(SO_3CF_3)_2$	$Ca(SO_3CF_3)_2$	$Ba(SO_3CF_3)_2$	$Zn(SO_3CF_3)_2$	$Cu(SO_3CF_3)_2$
Temperature (K)	295	295	295	295	295
Formula weight (g mol^{-1})	322.43	338.20	435.45	363.50	361.670
Space group	$R\bar{3}$	$R\bar{3}$	$I2/a$†	$R\bar{3}$	$P\bar{1}$
Z	3	3	4	3	1
a (Å)	5.0494 (5)	5.60549 (3)	21.751 (1)	4.9787 (1)	4.9896 (2)
b (Å)	5.0494 (5)	5.60549 (3)	4.9080 (1)	4.9787 (1)	10.7668 (4)
c (Å)	31.033 (2)	31.1417 (2)	9.6949 (3)	31.3165 (7)	4.8219 (2)
α (°)	90	90	90	90	103.523 (3)
β (°)	90	90	100.379 (3)	90	118.085 (3)
γ (°)	120	120	90	120	79.459 (3)
V (Å^3)	685.23 (9)	847.42 (1)	1018.01 (8)	672.27 (2)	221.40 (1)
ρ_{calc} (g cm^{-3})	2.344	1.988	2.841	2.694	2.713
Wavelength (Å)	0.64899	0.69953	0.24804	0.24804	0.24804
Capillary diameter (mm)	0.5	0.5	0.5	0.5	0.5
R_p‡	0.1063	0.0764	0.08.28	0.0805	0.0886
R_{wp}‡	0.1395	0.1569	0.1141	0.1045	0.1231
R_{F^2}‡	0.1204	0.1607	0.1555	0.1101	0.2163
χ^2	2.077	5.257	2.080	1.131	1.666
No. reflections	181	119	515	233	737

† The non-standard setting of the monoclinic unit cell was chosen for better comparison to the other divalent trifluoromethyl sulfonates under investigation. Standard setting: $C2/c$, a = 22.147, b = 4.909, c = 21.732 Å, β = 154.49°. ‡ R_p, R_{wp} and R_{F^2} as defined in *GSAS* (Larson & Von Dreele, 2002).

studies, the dynamics of anions as well as cations, and their interactions, have been investigated by two independent probes, impedance spectroscopy and solid-state NMR (van Wüllen *et al.*, 2004, 2005). For the two compounds investigated in depth, $LiSO_3CF_3$ and $NaSO_3CF_3$, a strong correlation between rotational-anion and translational-cation mobility has been evidenced. However, in spite of the rich dynamics observed, the ionic conductivities are not high enough for a technical application. Very low concentrations of intrinsic defects of these virtually stoichiometric phases explain this deficiency. A straightforward way of improving the ionic conductivities would be to create extrinsic defects in the cation sublattice by aliovalent doping with trifluoromethyl sulfonates of divalent cations. For this purpose at least parts of the quasi-binary systems $M^+SO_3CF_3/M^{2+}(SO_3CF_3)_2$ need to be explored. In searching the literature for some relevant data on the trifluoromethyl sulfonates of divalent metals, we could not find any entry except for unindexed powder diffraction data of $Mg(SO_3CF_3)_2$ (Gill *et al.*, 1987), vibrational spectroscopy and EXAFS analysis of $Cu(SO_3CF_3)_2$ (Boumizane *et al.*, 1991) and the melting points and conductivity measurements in organic solvents of $Cu(SO_3CF_3)_2$ (Takei, 1984) and $Zn(SO_3CF_3)_2$ (Takei, 1985). Since we regarded basic knowledge of the pure border phases as a necessary precondition for our doping experiments, we have prepared the anhydrous salts $M(SO_3CF_3)_2$ (M = Mg, Ca, Ba, Zn, Cu) and have determined their crystal structures from synchrotron X-ray powder diffraction data.

2. Experimental

2.1. Synthesis

The trifluoromethyl sulfonates of divalent cations $M(SO_3CF_3)_2$ (M = Mg, Ca, Ba, Zn, Cu) were purchased from Aldrich. For purification the salts were recrystallized from water and dried under vacuum for three days at T = 403 K. We also prepared $Mg_{0.96}Na_{0.08}(SO_3CF_3)_2$ by heating a mixture of 299 mg $Mg(SO_3CF_3)_2$ and 47 mg $NaSO_3CF_3$ to 523 K for 80 h under dry argon. $NaSO_3CF_3$ was prepared by neutralization of CF_3SO_3H (0.3 *M*, 99+%, Aldrich) with NaOH (p.a., Fluka) in aqueous solution. The precipitate, identified as the monohydrate $NaSO_3CF_3.H_2O$, was transformed into the final product by heating *in vacuo* at T = 473 K for one month. The purity of the samples was checked using laboratory X-ray powder diffraction and infrared spectroscopy.

2.2. X-ray powder diffraction

High-resolution powder diffraction patterns at room temperature were collected in Debye–Scherrer mode at the high-resolution powder diffractometer at ID31 of the European Synchrotron Radiation Facility (ESRF) for Zn-, Ba- and Cu-trifluoromethyl sulfonate and on beamline X3B1 of the Brookhaven National Synchrotron Light Source for Mg-, $Mg_{0.96}Na_{0.08}$- and Ca-trifluoromethyl sulfonate. The samples were sealed in lithium borate glass capillaries of diameter 0.5 mm (Hilgenberg glass No. 50) and rotated around θ in order to improve the spatial averaging. A Si 111 reflection was used to select X-ray energies of 49.98 keV (for Zn-, Ba- and Cu-trifluoromethyl sulfonate), 17.7 keV (for Ca-trifluoromethyl sulfonate) and 19.07 keV for Mg-trifluoromethyl sulfonate. The exact wavelength and the zero point were determined from well defined reflections of a silicon standard (ID31) and of the NBS1976 flat-plate alumina standard (X3B1). At X3B1, the diffracted beam was analyzed with a Ge(111) crystal and detected with a Na(Tl)I scintillation counter. At ID31, nine crystal analyzers [nine Ge(111) crystals separated by 2° intervals] with nine Na(Tl)I scintillation counters were used simultaneously. The incoming beam was monitored using an ion chamber for normalization purposes in order to take the decay of the primary beam into account.

At X3B1 data were collected in step-scan mode, while at ID31 20 min scans were recorded in continuous mode for several hours and later normalized and converted to step-scan data in steps of 0.002°. Severe radiation damage, resulting in anisotropic peak shift and broadening, started after exposure times of >20 min at ID31 which made it necessary to translate the sample to an unexposed area every 20 min during data collection.

Data reduction on the high-resolution powder diffraction patterns was performed using *GUFI* (Dinnebier & Finger, 1998). Indexing with *ITO* (Visser, 1969) led to rhombohedral unit cells for Ca-, $Mg_{0.96}Na_{0.08}$- and Zn-trifluoromethyl sulfonate, to an I(C)-centred monoclinic unit cell for Ba-trifluoromethyl sulfonate, and to a triclinic unit cell for Cu-trifluoromethyl sulfonate with lattice parameters given in Table 1. The non-standard setting of the monoclinic unit cell of Ba-trifluoromethyl sulfonate was chosen for better comparison with the other bivalent trifluoromethyl sulfonates under investigation. Application of the extinction rules revealed $R3$, $R\bar{3}$, $R3m$, $R\bar{3}m$, $I2/a(C2/c)$, $P1$ and $P\bar{1}$ as the most probable space groups. The number of formula units per unit cell was calculated from volume increments. The peak profiles and precise lattice parameters for all powder patterns were determined by LeBail-type fits (Le Bail *et al.*, 1988) using the program *GSAS* (Larson & Von Dreele, 2002). The background was modelled manually using *GUFI*. The peak profile was described by a pseudo-Voigt function in combination with a special function that accounts for the asymmetry due to axial divergence (Thompson *et al.*, 1987; Finger *et al.*, 1994). The powder patterns of the Ca-, Zn-, Ba-, Mg- and $Mg_{0.96}Na_{0.08}$-trifluoromethyl sulfonates exhibit some anisotropic peak broadening caused by lattice strain. The phenomenological strain model of Stephens (1999) as implemented in *GSAS* was used to model the anisotropy of the FWHM. Four parameters were refined for the rhombohedral lattices and nine parameters for the monoclinic lattices.

The crystal structures of all investigated trifluoromethyl sulfonates were solved by global optimization in direct space using the *DASH* structure solution package (David *et al.*, 1998). The measured powder patterns at room temperature were subjected to Pawley refinements (Pawley, 1981) in all possible space groups in order to extract correlated integrated intensities from the patterns. Good fits to the data were obtained. An internal coordinate description of the $(SO_3CF_3)^-$ moiety was constructed using bond lengths, angles and torsion angles from corresponding lithium trifluoromethyl sulfonate (Tremayne *et al.*, 1992). The position of the divalent cation as well as the position and orientation of the $(SO_3CF_3)^-$ anion in the unit cell were postulated and the trial structures were subjected to a global optimization. The structures giving the best fit to the data in space groups $R\bar{3}$ (Zn-, Mg-, Ca-trifluoromethyl sulfonate), $I2/a(C2/c)$ (Ba-trifluoromethyl sulfonate) and $P\bar{1}$ (Cu-trifluoromethyl sulfonate) were validated by Rietveld refinement (Rietveld, 1969) of the fractional coordinates obtained at the end of the simulated annealing run using the *GSAS* program.

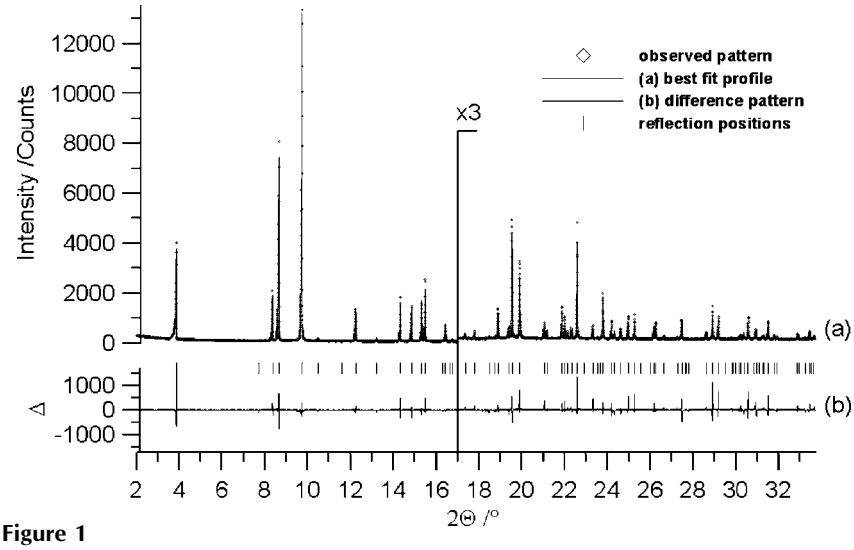

Figure 1
Scattered X-ray intensities for $Ca(SO_3CF_3)_2$ at T = 295 K as a function of diffraction angle 2θ. Shown are the observed patterns (diamonds), the best Rietveld-fit profiles (line) and the difference curve between observed and calculated profiles (below). The high-angle part starting at 17° 2θ is enlarged. The diffraction patterns and Rietveld-fit profiles for Mg-, Ba-, Zn- and Cu-trifluoromethyl sulfonate are given in the supplementary material.

To stabilize the refinements of the $(SO_3CF_3)^-$ anion, either soft constraints for the bond lengths (C—S, C—F, S—O) and bond angles (S—C—F, C—S—O) or rigid bodies employing TLS matrices were introduced (Dinnebier, 1999). The crystallinity of magnesium trifluoromethyl sulfonate was not sufficient for crystal structure determination. We found that the addition of a small amount of sodium trifluoromethyl sulfonate highly increases the quality of the diffraction data without major changes in position and relative intensity of the reflexes. Therefore we used $Mg_{0.96}Na_{0.08}(SO_3CF_3)_2$ to determine the unit cell and to solve the crystal structure. The identity of the crystal structure of sodium-free magnesium trifluoromethyl sulfonate was then validated by Rietveld refinement. Nevertheless, the powder patterns of Mg-, Ba- and Cu-trifluoromethyl sulfonate exhibit a certain degree of structural defects, visible in background humps and odd line-shapes.

3. Results and discussion

3.1. Crystal structure

The crystal structures of $M(SO_3CF_3)_2$ (M = Mg, Ca, Ba, Zn, Cu) have been determined from high-resolution X-ray powder diffraction data (Fig. 1). The agreement factors (R values) are listed in Table 1, and the coordinates and displacement parameters are given in the supplementary material.[1] A

[1] Supplementary data for this paper are available from the IUCr electronic archives (Reference: SN5032). Services for accessing these data are described at the back of the journal.

Table 2
Some structural data (distances in Å and angles in °) for calcium, magnesium, zinc, barium and copper trifluoromethyl sulfonate at T = 295 K.

Formula	$Ca(SO_3CF_3)_2$	$Mg(SO_3CF_3)_2$	$Zn(SO_3CF_3)_2$	$Cu(SO_3CF_3)_2$	$Ba(SO_3CF_3)_2$
S—C	1.820 (2)	1.821	1.820 (2)	1.790 (5)	1.809 (6)
S—O	1.445 (10)	1.445 (10)	1.445 (3)	1.460 (10)	1.43 (1)–1.45 (1)
C—F	1.302 (7)	1.30 (1)	1.302 (3)	1.33 (1)	1.31 (1)
O—S—O	109.5 (3)	109.5 (5)	109.5 (1)	109.5 (5)	108.2 (7)–111.5 (7)
F—C—F	109.5 (3)	109.5 (5)	109.5 (2)	109.5 (6)	108.6 (8)–110.8 (8)

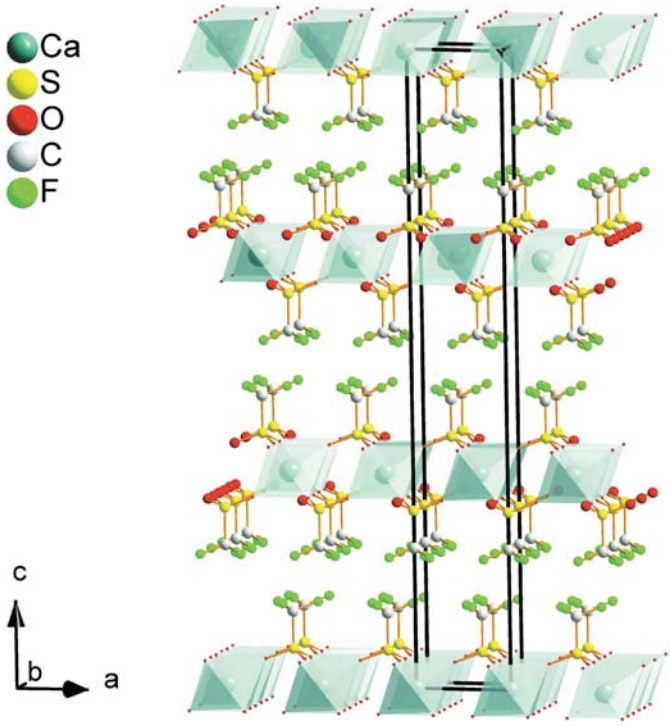

Figure 2
Crystal structure of the rhombohedral $Ca(SO_3CF_3)_2$ viewed along [010]. The structures of $Mg(SO_3CF_3)_2$ and $Zn(SO_3CF_3)_2$ are similar to this structure.

selection of intramolecular and intermolecular distances and angles is given in Table 2.

Like the alkali trifluoromethyl sulfonates (with the exception of potassium trifluoromethyl sulfonate), the crystal structures of $M(SO_3CF_3)_2$ (M = Mg, Ca, Ba, Zn, Cu) consist of double layers of trifluoromethyl sulfonate anions, with the lipophilic CF_3 groups pointing towards each other (Figs. 2, 3 and 4). The conformation of the trifluoromethyl sulfonate anions is staggered in the same way as is known for lithium, sodium, potassium and caesium trifluoromethyl sulfonate. The cations are located between SO_3 layers, as for all known alkali trifluoromethyl sulfonates.

In Mg-, Ca- and Zn-trifluoromethyl sulfonate the cations are coordinated octahedrally by O atoms [d(Mg—O) 2.029 (7) Å; d(Ca—O) 2.255 (6) Å; d(Zn—O) 2.069 (2) Å] (Fig. 5). In Cu-trifluoromethyl sulfonate the metal is coordinated by a Jahn–Teller distorted oxygen octahedron [d(Cu—O_{ax}) 2.280 (6) Å; d(Cu—O_{equ}) 1.928 (9)–1.981 (7) Å] (Fig. 6). This is in good agreement with earlier publications regarding EXAFS spectroscopy on Cu-trifluoromethyl sulfonate (Boumizane *et al.*, 1991). Boumizane *et al.* found a '4 + 2' oxygen coordination around the Cu atom with a Cu—O distance of 1.96 Å within the square planar environment. In barium trifluoromethyl sulfonate the metal atom is coordinated by eight O atoms [d(Ba—O) 2.70 (1)–2.98 (1) Å] (Fig. 7).

Visual inspection of Figs. 6, 7 and 8 immediately reveals that the crystal structures of all investigated bivalent trifluoromethyl sulfonates are related to each other. To understand the principles of crystal packing and to compare the different crystal structures of $M(SO_3CF_3)_2$ (M = Mg, Ca, Ba, Zn, Cu), the trifluoromethyl sulfonate ions are replaced by their barycentres X^-. In principle, two different (idealized) anionic packings are realised: in the magnesium (and isostructural calcium, zinc) and the copper salts (Fig. 8), (pseudo)hexagonal double layers

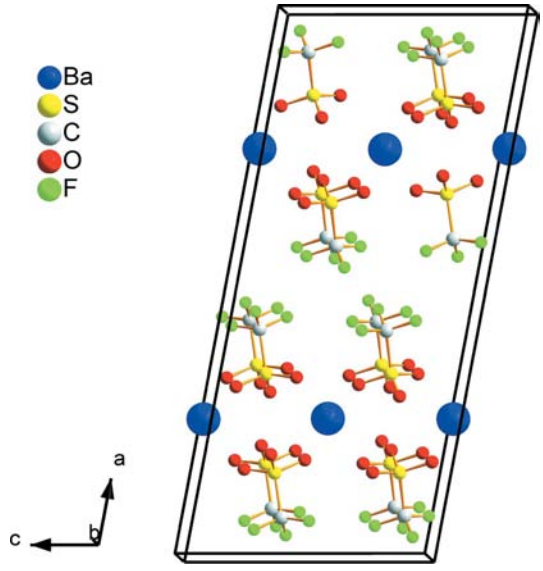

Figure 3
Crystal structure of monoclinic $Ba(SO_3CF_3)_2$ viewed along [010].

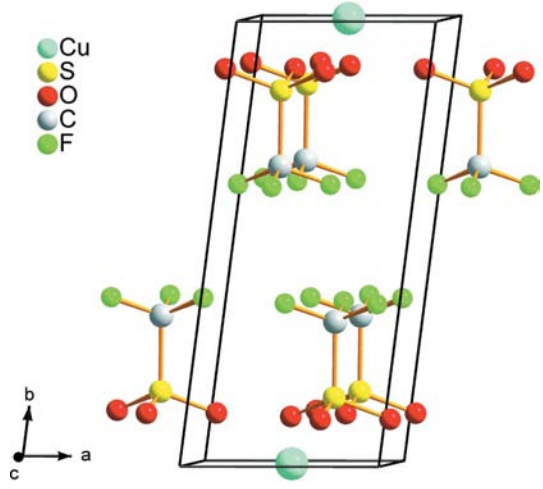

Figure 4
Crystal structure of $Cu(SO_3CF_3)_2$ viewed along [001].

showing an $AB_2^{IV}M^{VI}$-type packing of edge-linked $M^{2+}X_6^{1-}$ octahedra are formed. These octahedra are lying on one of their triangular faces sharing six out of twelve edges with neighbouring octahedra. In calcium, magnesium and zinc trifluoromethyl sulfonate, these layers are arranged perpendicular to the *c*-axis, while in copper trifluoromethyl sulfonate the layers are arranged perpendicular to the *b** axis. Consecutive layers are shifted with regard to each other with a period of approximately four (calcium trifluoromethyl sulfonate) and three (copper trifluoromethyl sulfonate) layers. There exists a direct maximal supergroup–subgroup relation between the rhombohedral space group $R\bar{3}$ of calcium, magnesium and zinc trifluoromethyl sulfonate and the triclinic space group $P\bar{1}$ of copper trifluoromethyl sulfonate.

In barium trifluoromethyl sulfonate, (pseudo)cubic layers showing an AAM^{VIII}-type packing of face-linked $M^{2+}X_8^{1-}$ cubes are formed (Fig. 9). These cubes share four out of six faces with neighbouring cubes forming layers perpendicular to the *a** axis. The period between consecutive layers is four.

Since the differences between the two principal types of crystal packings are mainly due to the locations and orientations of the trifluoromethyl sulfonate ions, it is generally possible to derive all three types of unit cells from the cationic packing, as illustrated for Ca-trifluoromethyl sulfonate in Fig. 10, where the transformation operators (including the translational part) are

$$\begin{pmatrix} \bar{1} & 2/3 & 2/3 & 5/6 \\ \bar{1} & 0 & 0 & -5/6 \\ 0 & \bar{2} & 0 & 1/6 \\ 0 & 0 & 0 & 1 \end{pmatrix}$$

from the rhombohedral to the monoclinic unit cell and

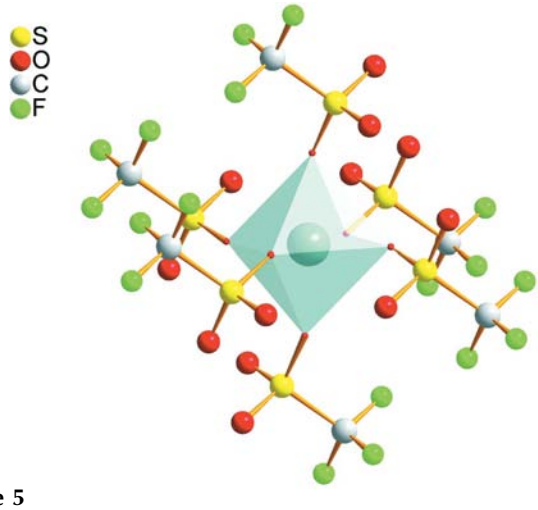

Figure 5
Octahedral coordination of the cation in $Ca(SO_3CF_3)_2$. The coordination in $Mg(SO_3CF_3)_2$ and $Zn(SO_3CF_3)_2$ are similar to this picture.

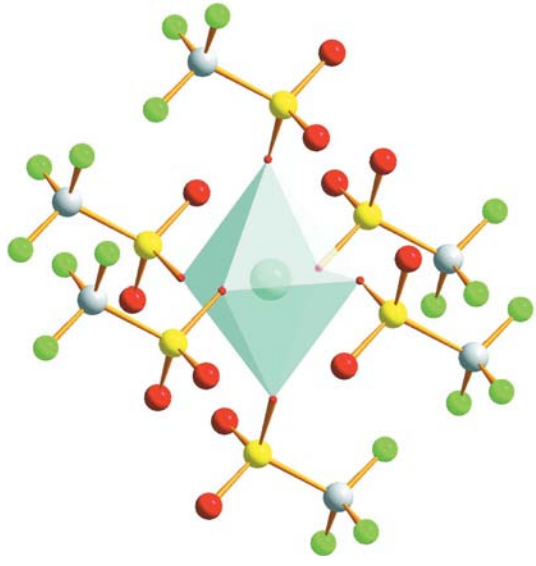

Figure 6
Jahn–Teller distorted oxygen octahedron around the copper ion in $Cu(SO_3CF_3)_2$.

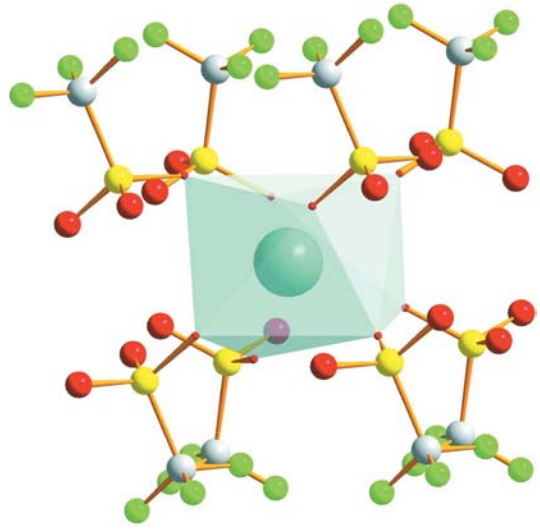

Figure 7
Barium ion in $Ba(SO_3CF_3)_2$, coordinated by eight O atoms.

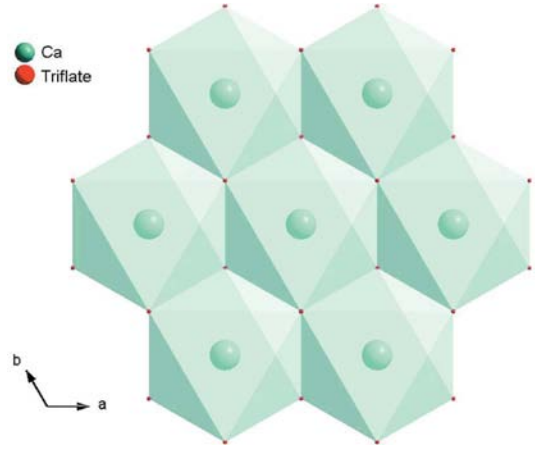

Figure 8
Crystal packing of one layer of $Ca(SO_3CF_3)_2$ with the trifluoromethyl sulfonate ions drawn as balls around their centre of gravity. The packing of $Ca(SO_3CF_3)_2$, $Zn(SO_3CF_3)_2$ and $Cu(SO_3CF_3)_2$ are similar to this picture.

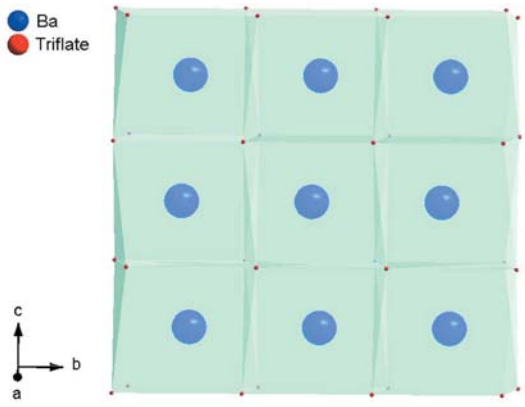

Figure 9
Crystal packing of one layer of $Ba(SO_3CF_3)_2$ with the trifluoromethyl sulfonate ions drawn as balls around their centre of gravity.

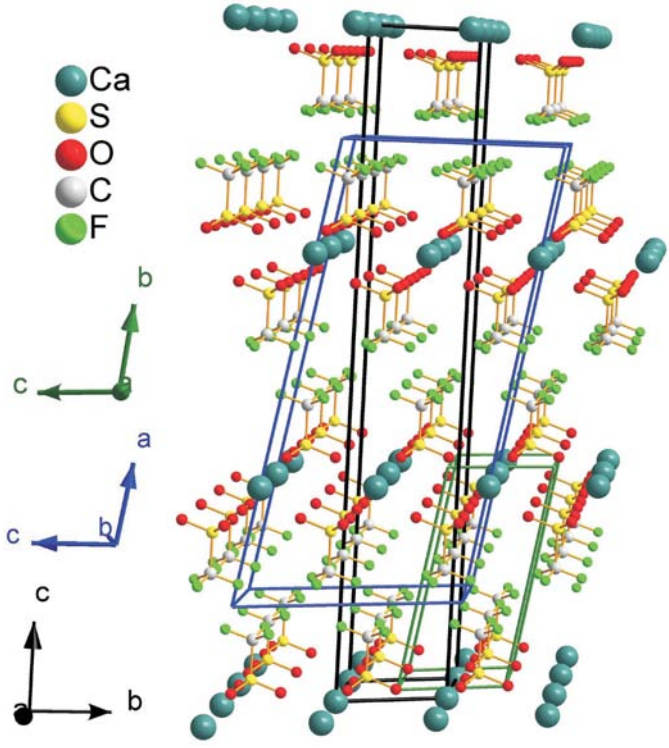

Figure 10
The hexagonal (black lines), monoclinic (blue lines) and triclinic (green lines) unit cells, shown in relation to the crystal structure of $Ca(SO_3CF_3)_2$.

$$\begin{pmatrix} 1 & 0 & 0 & 1/2 \\ -1/3 & 1/3 & 1/3 & 1/2 \\ 0 & \bar{1} & 0 & 0 \\ 0 & 0 & 0 & 1 \end{pmatrix}$$

from the rhombohedral to the triclinic unit cell.

4. Conclusion

It was found that the divalent metal salts of trifluoromethyl sulfonic acid $M(SO_3CF_3)_2$ (M = Mg, Ca, Ba, Zn, Cu) adopt a layered arrangement. Depending on the space requirement of the cations, two different kinds of packing can be found. Owing to the fact that layered structures often show stacking disorder, the growth of single crystals, suitable for structure determination, proves difficult. High-resolution X-ray powder diffraction was essential for the solution of the crystal structures of the divalent trifluoromethyl sulfonates.

References

Boumizane, K., Herzog-Cance, M. H., Jones, D. J., Pascal, J. L., Potier, J. & Roziere, J. (1991). *Polyhedron*, **10**, 2757–2769.
David, W. I. F., Shankland, K. & Shankland, N. (1998). *Chem. Commun.* pp. 931–932.
Dinnebier, R. (1999). *Powder Diffr.* **14**, 84–92.
Dinnebier, R. E. & Finger, L. (1998). *Z. Kristallogr. Suppl.* **15**, 148.
Dinnebier, R. E., Sofina, N. & Jansen, M. (2004). *Z. Anorg. Allg. Chem.* **630**, 1613–1616.
Finger, L. W., Cox, D. E. & Jephcoat, A. P. (1994). *J. Appl. Cryst.* **27**, 892–900.
Forsyth, M., Tipton, A. L. & Shriver, D. F. (1997). *Solid State Ion.* **99**, 257.
Gill, M. S., Sethi, A. K. & Verma, R. D. (1987). *Can. J. Chem.* **65**, 409–411.
Greenbaum, S. G. (1987). *Mol. Cryst. Liq. Cryst.* **160**, 347.
Hildebrandt, L., Dinnebier, R. & Jansen, M. (2005). *Z. Anorg. Allg. Chem.* **631**, 1660–1666.
Ikeda, S., Mori, K., Furuhashi, Y. & Masuda, H. (1999). *Solid State Ion.* **121**, 329–333.
Ikeda, S., Mori, K., Furuhashi, Y., Masuda, H. & Yamamoto, O. (1999). *J. Power Sources*, **82**, 720–723.
Jansen, M. (1991). *Angew. Chem.* **103**, 1574; *Angew. Chem. Int. Ed. Engl.* **1530**, 1547.
Korus, G. & Jansen, M. (2001). *Z. Anorg. Allg. Chem.* **627**, 1599–1605.
Kumar, G. G. & Munichandraiah, N. (2000*a*). *J. Power Sources*, **91**, 157–160.
Kumar, G. G. & Munichandraiah, N. (2000*b*). *Solid State Ion.* **128**, 203–210.
Kumar, G. G. & Sampath, S. (2003). *Solid State Ion.* **160**, 289–300.
Kvist, A. & Bengtzelius, A. (1973). *Fast Ion Transport in Solids, Solid State Batteries and Devices*, edited by W. v. Gool, p. 193. Amsterdam: North Holland.
Larson, A. C. & Von Dreele, R. B. (2002). *GSAS 1994*, 2002 Version. Los Alamos National Laboratory, New Mexico, USA.
Le Bail, A., Duroy, H. & Fourquet, J. L. (1988). *Mater. Res. Bull.* **23**, 447–452.
Lundén, A. (1994). *Solid State Ion.* **68**, 77–80.
McLin, M. G. & Angell, C. A. (1992). *Solid State Ion.* **53–56**, 1027.
Mitra, S., Shukla, A. K. & Sampath, S. (2001). *J. Power Sources*, **101**, 213–218.
Mouhtady, O., Gaspard-Iloughmane, H., Roques, N. & Le Roux, C. (2003). *Tetrahedron Lett.* **44**, 6379–6382.
Munshi, M. Z. A., Gilmour, A., Smyri, W. H. & Owens, B. B. (1989). *J. Electrochem. Soc.* **136**, 1847.
Pawley, G. S. (1981). *J. Appl. Cryst.* **14**, 357–361.
Rhodes, C. P., Khan, M. & Frech, R. (2002). *J. Phys. Chem. B*, **106**, 10330.
Rhodes, C. P., Kiassen, B., Frech, R., Dai, Y. & Greenbaum, S. G. (1999). *Solid State Ion.* **126**, 251–257.
Rietveld, H. M. (1969). *J. Appl. Cryst.* **2**, 65–71.
Sage, V., Clark, J. H. & Macquarrie, D. (2004). *J. Catal.* **227.**
Secco, E. A. (1992). *J. Solid State Chem.* **96**, 366–375.
Secco, E. A. (1993). *Solid State Ion.* **60**, 233–235.
Semkow, W. K. & Sammels, A. F. (1987). *J. Electrochem. Soc.* **134**, 766.
Sofina, N., Peters, E. M. & Jansen, M. (2003). *Z. Anorg. Allg. Chem.* **629**, 1431–1436.
Stephens, P. W. (1999). *J. Appl. Cryst.* **32**, 281–289.

Takei, T. (1984). *Surf. Technol.* **22**, 343–352.
Takei, T. (1985). *Surf. Technol.* **25**, 369–375.
Thompson, P., Cox, D. E. & Hastings, J. B. (1987). *J. Appl. Cryst.* **20**, 79–83.
Tremayne, M., Lightfoot, P., Mehta, M. A., Bruce, P. G., Harris, K. D. M., Shankland, K., Gilmore, C. J. & Bricogne, G. (1992). *J. Solid State Chem.* **100**, 191–196.
Umenoto, T., Tomita, K. & Kawada, K. (1990). *Org. Synth.* **69**, 129.
Visser, J. W. (1969). *J. Appl. Cryst.* **2**, 89–95.
Wüllen, L. van, Hildebrandt, L. & Jansen, M. (2005). *Solid State Ion.* **176**, 1449–1456.
Wüllen, L. van, Sofina, N. & Jansen, M. (2004). *Chem. Phys. Chem.* **5**, 1906–1911.
Zheng, Y., Bhatt, D. & Davis, F. (1998). *Thin Solid Films*, **327**, 473.